

# Reduction of Torque Ripple in DTC for Induction Motor Using Input–Output Feedback Linearization

Sebti Belkacem<sup>1</sup>, Farid Naceri<sup>1</sup>, Rachid Abdessemed<sup>2</sup>

**Abstract:** Direct torque control (DTC) is known to produce fast response and robust control in AC adjustable-speed drives. However, in the steady-state operation, notable torque, flux, and current pulsations occur. In this paper a nonlinear DTC of IM drives is presented based on a Space Vector PWM scheme combined with Input–Output Feedback Linearization (IOFL) technique. The variation of stator and rotor resistance due to changes in temperature or frequency deteriorates the performance of DTC controller by introducing errors in the estimated flux linkage and the electromagnetic torque. As a result, this approach will not be suitable for high power drives such as those used in tractions, as they require good torque control performance at considerably lower frequency. Finally, extensive simulation results are presented to validate the proposed technique. The system is tested at different speeds and a very satisfactory performance has been achieved.

**Keywords:** DTC-SVPWM, Key parameters variation, Robustness, Input–output feedback linearization.

## 1 Introduction

Today Direct Torque Control (DTC) and NonLinear Control (NLC) are considered the most important techniques to achieve high dynamic performance in AC machines. The direct torque control (DTC) scheme has been increased due to several factors such as quick torque response and robustness against the motor parameter variations [1]. The conventional DTC algorithm using the hysteresis based voltage switching method has relative merits of simple structure and easy implementation. The performance of such a scheme depends on the error band set between the desired and measured torque and stator flux values. In addition, in this control scheme, the inverter switching frequency is changed according to the hysteresis bandwidth of flux and torque controllers and the variation of speed and motor parameters. Superior motor performance is achieved by narrower hysteresis bands especially in the high-speed region. As a result, this approach will not be suitable for high power drives such as those

---

<sup>1</sup>Department of Electrical Engineering, University of Batna, 05000, Algeria; E-mail: belkacem\_sebti@yahoo.fr

<sup>2</sup>LEB, Department of Electrical Engineering, University of Batna, 05000, Algeria

used in tractions, as they require good torque control performance at considerably lower frequency.

To overcome the drawbacks problems, although several methods to solve these problems have been presented [2-13], the control scheme in [6] is sensitive to parameters uncertainty, especially to the stator resistance variations, and the stability will be affected by parameter variation and the system model must be known. Otherwise, the system dynamic performance and stability will be significantly affected by parameter variations. To solve this problem, adaptive nonlinear control methods such as adaptive input–output feedback linearization technique, adaptive backstepping control technique, sliding mode and adaptive sliding mode control techniques have been applied to induction motor drives [14–20]. In these studies, an adaptation law is developed to compensate the parametric uncertainty of the stator and rotor resistance and the external load torque of the IM. The contribution of this paper is to describe a robust DTC-SVPWM method for a torque and flux control of induction motor drive based on input–output feedback linearization technique. Simulation results demonstrate the feasibility and validity of the proposed DTC system by effectively accelerating system response, reducing torque and flux ripple and a very satisfactory performance has been achieved.

## 2 Model Description and Control Design

The model of the IM expressed in the stationary “ $\alpha\beta$ ” axes reference frame can be expressed by

$$\begin{aligned} \frac{d i_{s\alpha}}{d t} &= -\left(\frac{R_s}{\sigma L_s} + \frac{R_r}{\sigma L_r}\right) i_{s\alpha} - \omega_r i_{s\beta} + \frac{R_r}{\sigma L_r L_s} \Phi_{s\alpha} + \frac{\omega_r}{\sigma L_s} \Phi_{s\beta} + \frac{1}{\sigma L_s} V_{s\alpha}, \\ \frac{d i_{s\beta}}{d t} &= -\left(\frac{R_s}{\sigma L_s} + \frac{R_r}{\sigma L_r}\right) i_{s\beta} + \omega_r i_{s\alpha} + \frac{R_r}{\sigma L_r L_s} \Phi_{s\beta} - \frac{\omega_r}{\sigma L_s} \Phi_{s\alpha} + \frac{1}{\sigma L_s} V_{s\beta}, \\ \frac{d \Phi_{s\alpha}}{d t} &= V_{s\alpha} - R_s i_{s\alpha}, \\ \frac{d \Phi_{s\beta}}{d t} &= V_{s\beta} - R_s i_{s\beta}, \end{aligned} \quad (1)$$

where  $i_s$ ,  $\Phi_s$ ,  $V_s$ ,  $R$  and  $L$  denote stator currents, stator flux, stator voltage, resistance and inductance, respectively,  $\omega_r$  denotes the rotor speed and  $M$  is the mutual inductance.  $\sigma = 1 - \frac{M^2}{L_s L_r}$  is the redefined leakage inductance.

The generated torque of the IM can be expressed in terms of stator currents and stator flux linkage as

$$T_e = \frac{3p}{2} (\Phi_{s\alpha} i_{s\beta} - \Phi_{s\beta} i_{s\alpha}), \quad (2)$$

where  $p$  is the number of pole pairs.

The mechanical dynamic equation is given by

$$\frac{d\omega_m}{dt} = \frac{3p}{2J} (\Phi_{s\alpha} i_{s\beta} - \Phi_{s\beta} i_{s\alpha}) - \frac{T_L}{J}, \quad (3)$$

where  $J$  and  $T_L$  denote the moment of inertia of the motor, the load torque and  $\omega_m$  is the rotor mechanical speed ( $\omega_r = p\omega_m$ ).

For the proposed nonlinear input-output feedback linearization controller, the state coordinate transformation is applied. Therefore, the state coordinate's transformed model from (1) can be rewritten in a compact form as

$$\begin{aligned} \dot{x} &= f(x) + g_1(x)V_{s\alpha} + g_2(x)V_{s\beta}, \\ y &= h(x), \end{aligned} \quad (4)$$

where  $x$  is defined as:

$$f(x) = \begin{bmatrix} -\left(\frac{R_s}{\sigma L_s} + \frac{R_r}{\sigma L_r}\right) i_{s\alpha} - \omega_r i_{s\beta} + \frac{R_r}{\sigma L_r L_s} \Phi_{s\alpha} + \frac{\omega_r}{\sigma L_s} \Phi_{s\beta} \\ -\left(\frac{R_s}{\sigma L_s} + \frac{R_r}{\sigma L_r}\right) i_{s\beta} + \omega_r i_{s\alpha} + \frac{R_r}{\sigma L_r L_s} \Phi_{s\beta} - \frac{\omega_r}{\sigma L_s} \Phi_{s\alpha} \\ -R_s i_{s\alpha} \\ -R_s i_{s\beta} \end{bmatrix}, \quad (5)$$

$$x = [i_{s\alpha}, i_{s\beta}, \Phi_{s\alpha}, \Phi_{s\beta}]^T,$$

$$g_1(x) = \begin{bmatrix} \frac{1}{\sigma L_s} & 0 & 1 & 0 \end{bmatrix}^T, \quad (6)$$

$$g_2(x) = \begin{bmatrix} 0 & \frac{1}{\sigma L_s} & 0 & 1 \end{bmatrix}^T.$$

The generated torque  $T_e$  and the squared modules of the stator flux linkage  $|\Phi_s|^2 = \Phi_{s\alpha}^2 + \Phi_{s\beta}^2$  are assumed to be the system outputs. Therefore, by considering

$$h_1(x) = T_e = \frac{3p}{2} (\Phi_{s\alpha} i_{s\beta} - \Phi_{s\beta} i_{s\alpha}), \quad (7)$$

$$h_2(x) = |\Phi_s|^2 = \Phi_{s\alpha}^2 + \Phi_{s\beta}^2.$$

Define the controller objectives  $y_1$  and  $y_2$  as

$$\begin{aligned} y_1 &= h_1(x), \\ y_2 &= h_2(x). \end{aligned} \quad (8)$$

### 3 IOFL Technique

To linearized the nonlinear model in (4), the controlled variable is differentiated with respect to time until the input appears. This can be easily done by introducing the Lie derivative.

#### 3.1 Degree relating to the torque

$$\dot{y}_1 = L_f h_1(x) + L_{g_1} h_1(x) V_{s\alpha} + L_{g_2} h_1(x) V_{s\beta}, \quad (9)$$

where

$$\begin{aligned} L_f h_1 &= -\frac{3p}{2} \Phi_{s\beta} \left[ -\left( \frac{R_s}{\sigma L_s} + \frac{R_r}{\sigma L_r} \right) i_{s\alpha} - \omega_r i_{s\beta} + \frac{\omega_r}{\sigma L_s} \Phi_{s\beta} \right] + \\ &+ \frac{3p}{2} \Phi_{s\alpha} \left[ -\left( \frac{R_s}{\sigma L_s} + \frac{R_r}{\sigma L_r} \right) i_{s\beta} + \omega_r i_{s\alpha} - \frac{\omega_r}{\sigma L_s} \Phi_{s\alpha} \right], \\ L_{g_1} h_1 &= \frac{3p}{2} \left( i_{s\beta} - \frac{1}{L_s \sigma} \Phi_{s\beta} \right), \\ L_{g_2} h_1 &= \frac{3p}{2} \left( \frac{1}{L_s \sigma} \Phi_{s\alpha} - i_{s\alpha} \right). \end{aligned}$$

#### 3.2 Degree relating to the flux

$$\dot{y}_2 = L_f h_2(x) + L_{g_1} h_2(x) V_{s\beta} + L_{g_2} h_2(x) V_{s\alpha}, \quad (10)$$

where

$$\begin{aligned} L_f h_2 &= -2R_s (\Phi_{s\alpha} i_{s\alpha} - \Phi_{s\beta} i_{s\beta}), \\ L_{g_1} h_2 &= 2\Phi_{s\alpha}, \\ L_{g_2} h_2 &= 2\Phi_{s\beta}. \end{aligned}$$

### 3.3 Nonlinear control law

The matrix defining the relation between the physical input  $u(x)$  and the output derivative  $y(x)$  is given by the expression (11).

$$\begin{bmatrix} \dot{y}_1 \\ \dot{y}_2 \end{bmatrix} = A(x) + E(x) \begin{bmatrix} V_{s\alpha} \\ V_{s\beta} \end{bmatrix}, \quad (11)$$

with

$$A(x) = \begin{bmatrix} L_f h_1 \\ L_f h_2 \end{bmatrix},$$

$$E(x) = \begin{bmatrix} \frac{3p}{2} \left( i_{s\beta} - \frac{1}{L_s \sigma} \Phi_{s\beta} \right) & \frac{3p}{2} \left( \frac{1}{L_s \sigma} \Phi_{s\alpha} - i_{s\alpha} \right) \\ 2\Phi_{s\alpha} & 2\Phi_{s\beta} \end{bmatrix}, \quad (12)$$

$$\det(E(x)) = -3p \frac{M}{\sigma L_s L_r} [\Phi_{s\beta} \Phi_{r\beta} + \Phi_{s\alpha} \Phi_{r\alpha}]. \quad (13)$$

The matrix  $E(x)$  is reversible, the product of stator flux and rotor flux can not be equal to zero the following input-output feedback linearization is introduced for the system shown in (4)

$$\begin{bmatrix} V_{s\alpha} \\ V_{s\beta} \end{bmatrix} = E^{-1}(x) \left[ -A(x) + \begin{bmatrix} V_1 \\ V_2 \end{bmatrix} \right]. \quad (14)$$

## 4 Trajectory Imposition Control

The inputs  $V_1$ ,  $V_2$  can be calculated by [14, 15]. To ensure a perfect regulation and track the desired signals of the flux and torque towards their reference,  $V_1$ ,  $V_2$  are chosen as follows:

$$\begin{cases} V_1 = |\dot{\Phi}_s|_{ref}^2 + k_1 \left( |\Phi_s|_{ref}^2 - |\Phi_s|^2 \right), \\ V_2 = \dot{T}_{e ref} + k_2 (T_{e ref} - T_e), \end{cases} \quad (15)$$

where subscript ‘ref’ denotes the reference value.  $(k_1, k_2)$  are constant design parameters to be determined in order to make the decoupled system (15) stable.

The behavior of the linearized model is imposed by the poles placement methods. These coefficients are selected such as the equation  $s + k_1$ ,  $s + k_2$  are selected to satisfy the polynomial of Hurwitz.

## 5 Voltage Space Vector PWM

The voltage vectors, produced by a 3-phase PWM inverter, divide the space vector plane into six sectors as shown in Fig. 1

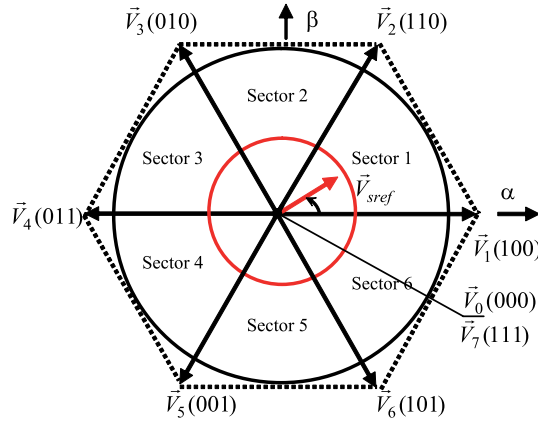


**Fig. 1** – The diagram of voltage space vectors.

In every sector, each voltage vector is synthesized by basic space voltage vector of the two side of sector and one zero vector. For example, in the first sector,  $\vec{V}_{sref}$  is a synthesized voltage space vector and expressed by:

$$\vec{V}_{sref} T_s = \vec{V}_0 T_0 + \vec{V}_1 T_1 + \vec{V}_2 T_2,$$

$$T_s = T_0 + T_1 + T_2,$$

where  $T_0, T_1$  and  $T_2$  are the work times of basic space voltage vectors  $\vec{V}_0, \vec{V}_1$  and  $\vec{V}_2$  respectively.

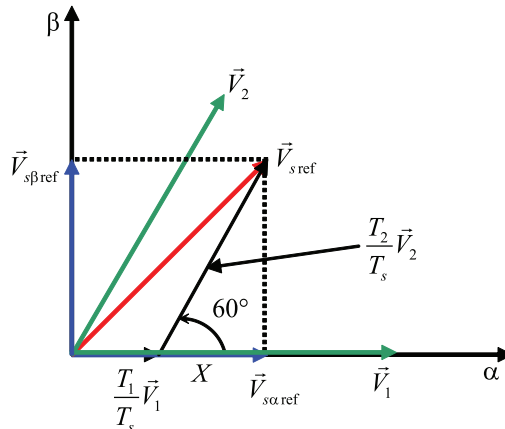


**Fig. 2** – Projection of the reference voltage vector.

## 6 Sensitivity Study and Simulation Results

In this section, the effectiveness of the proposed algorithm for torque and flux control of an IM is verified by computer simulations. The specifications for the used induction motor are listed in **Table 1**. The block scheme of the investigated direct torque control with space vector modulation is presented in (Fig. 3). In this work, we applied a direct torque control associated with a nonlinear control based on input-output linearization, switch table and hysteresis controller have been eliminated, where hysteresis controller is substituted by input–output feedback linearization and switch table is substituted by SVPWM. This approach eliminates the influence of stator and rotor resistance variation due to temperature and frequency changes.

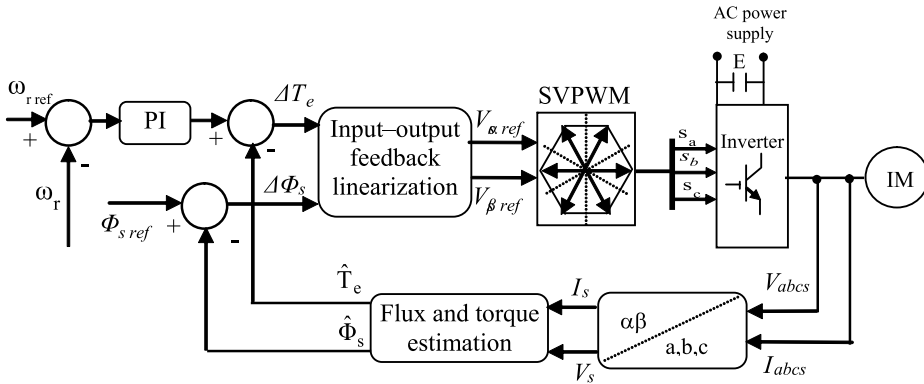


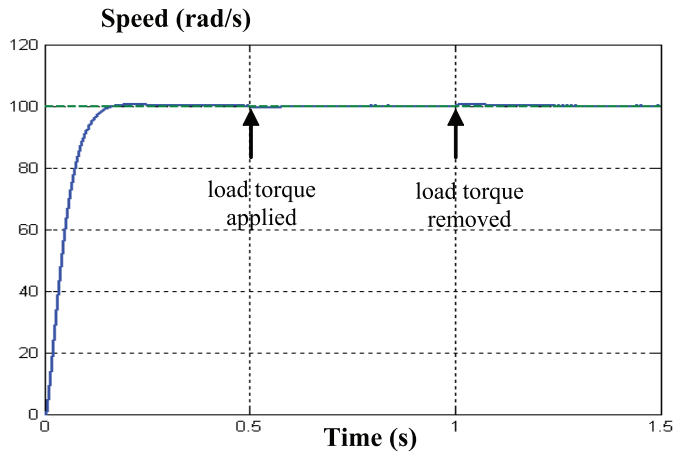
**Fig. 3** – Block diagram of the proposed DTC based on Input–output feedback linearization.

### 6.1 Variation of the load torque

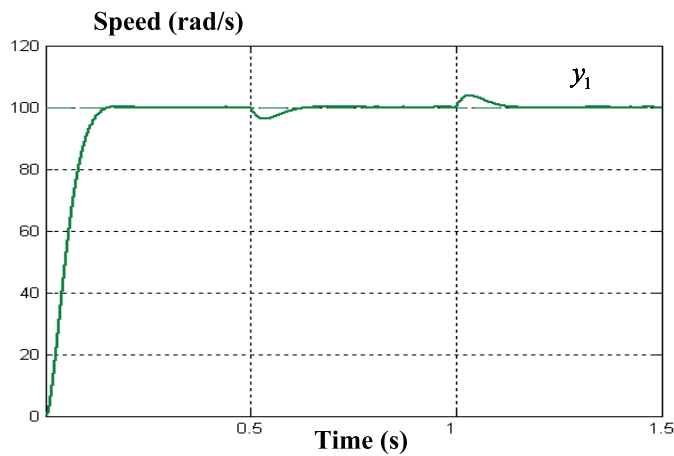
Fig. 4 shows the speed response of classical DTC and DTC based on IOFL controller's, The DTC-IOFL reacts faster than the classical DTC when load torque is suddenly applied and removed.

Moreover, the tracking performances are improved by the use of the DTC-IOFL law, in comparison with those of the classical DTC. These properties make the new algorithm suitable for applications where high tracking accuracy is required in the presence of external disturbances.

Current ripple has also a notable reduction in DTC-IOFL compared to classic DTC. In addition, a significantly lower ripple level in torque, flux see Fig. 5. Fig. 6 show the trajectory of the estimated stator flux components, the new DTC has good dynamic response as the classical control.



(a)



(b)

**Fig. 4** – Drive response under load torque change:

(a) DTC based IOFL, (b) Classical DTC.



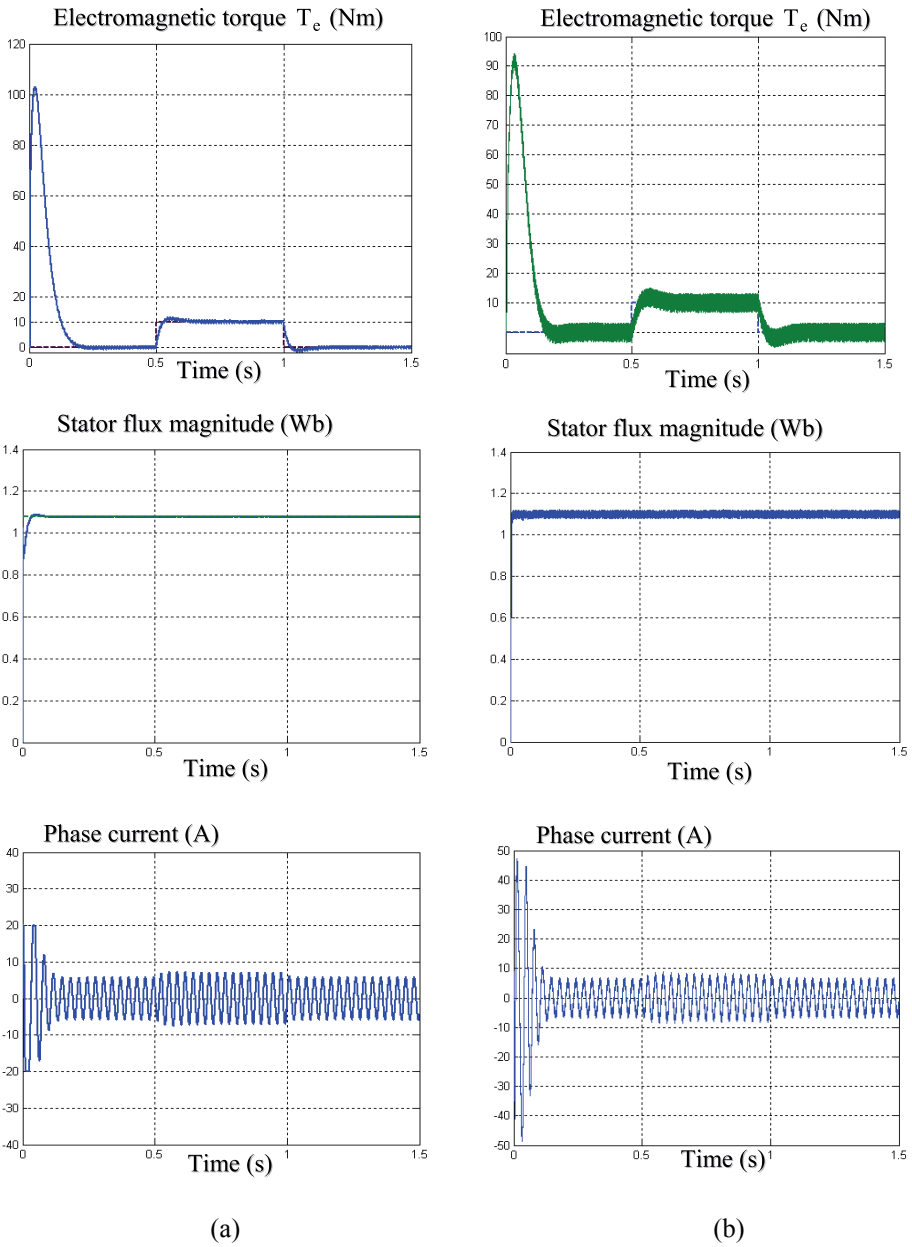


**Fig. 5** – Drive response under load torque change:  
 (a) DTC based IOFL; (b) Classical DTC.

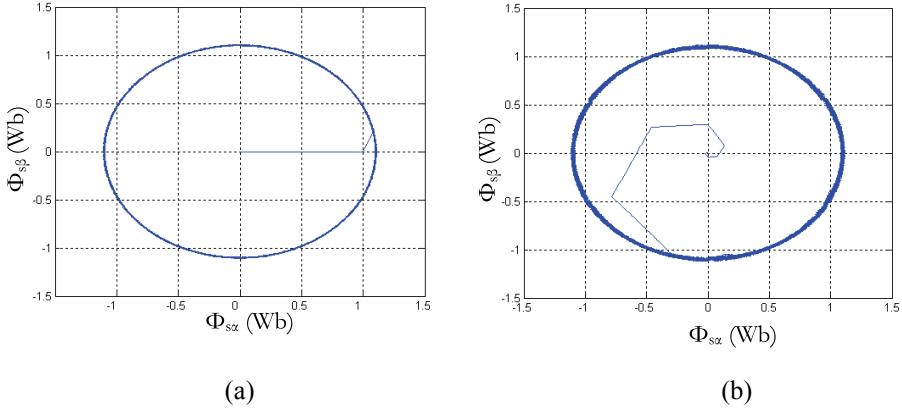


**Fig. 6** – Drive response under load torque change:  
 (a) DTC based IOFL; (b) Classical DTC.

**6.2 Variation in the stator resistance**

These tests investigate the influence of the electrical parameters change on the drive performance. Fig. 7 illustrate the simulation results of the process of speed estimation with a speed reference equal to 30 rad/s, after  $R_s$  increases by 50% and decreases by 50%, the variation in the stator resistance will not affect the controller performance. In the case of DTC-IOFL, the new algorithm show more robustness against stator resistance variation compared to the classical DTC.

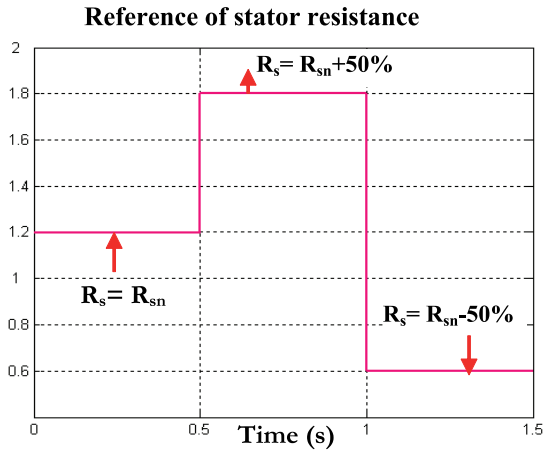


**Fig. 7a** – Drive response under variation of the stator’s resistance.

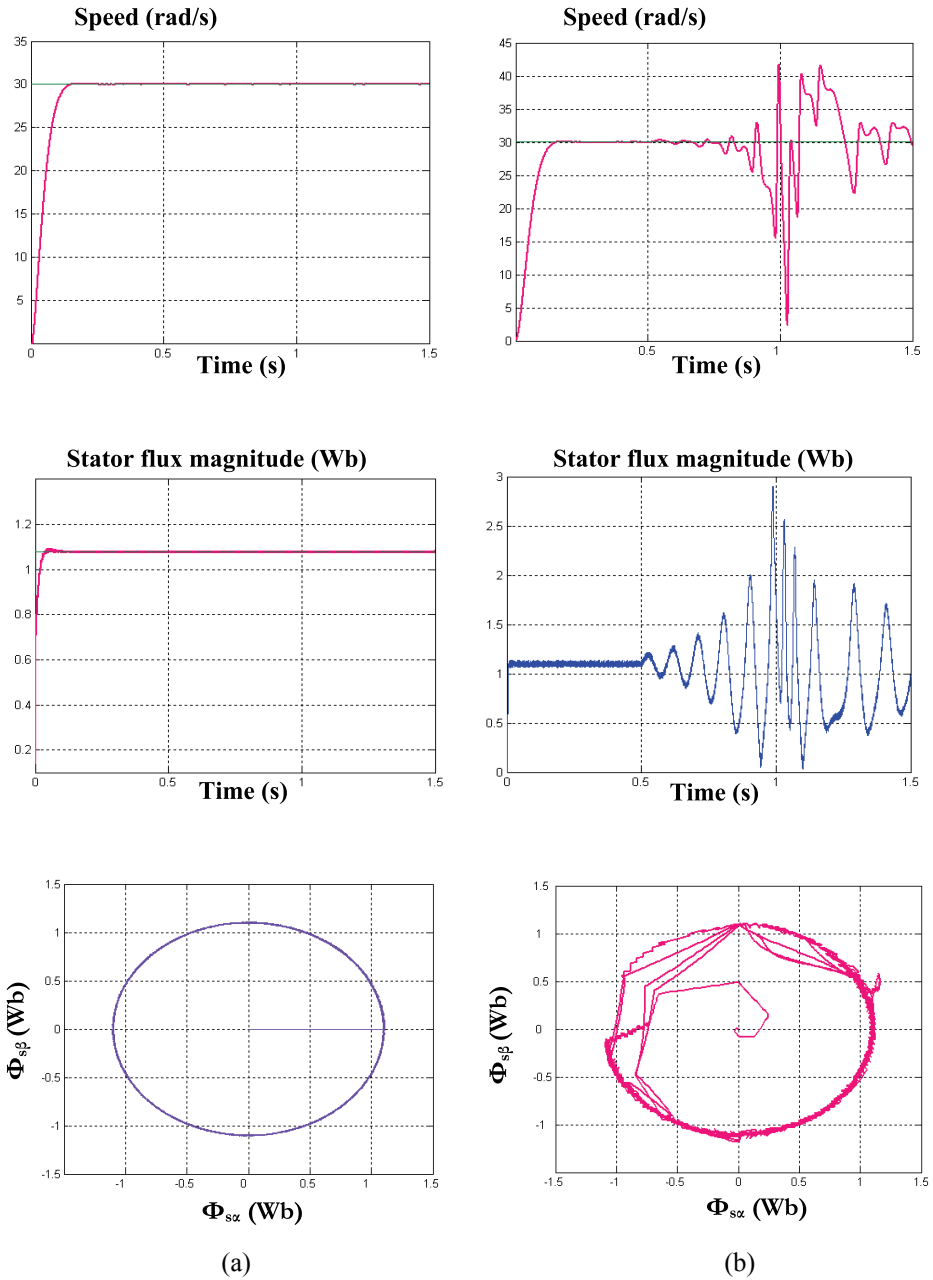


**Fig. 7b** – Drive response under variation of the stator's resistance:

(a) DTC based IOFL; (b) Classical DTC.

### 6.3 Variation in the inertia coefficient

Fig. 8 shows the drive dynamic under different values of inertia with constant speed reference. It is clear that the speed tracking is significantly unchanged, after  $J$  increases by 50% and decreases by 50%, for the new controlled compared to the classical controller.

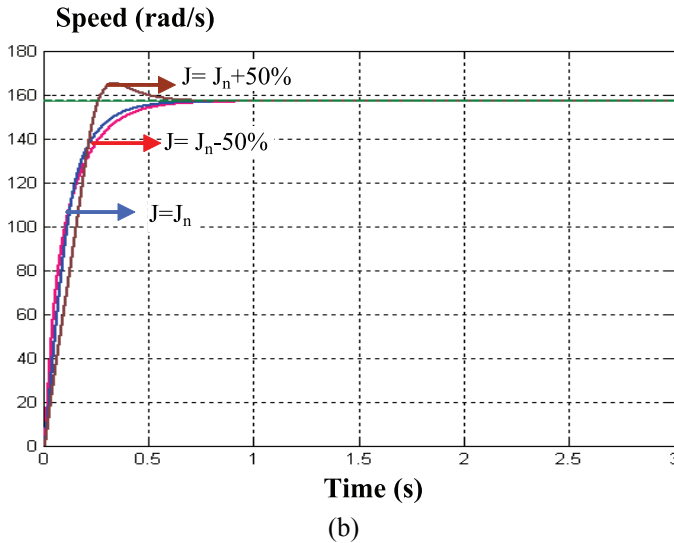
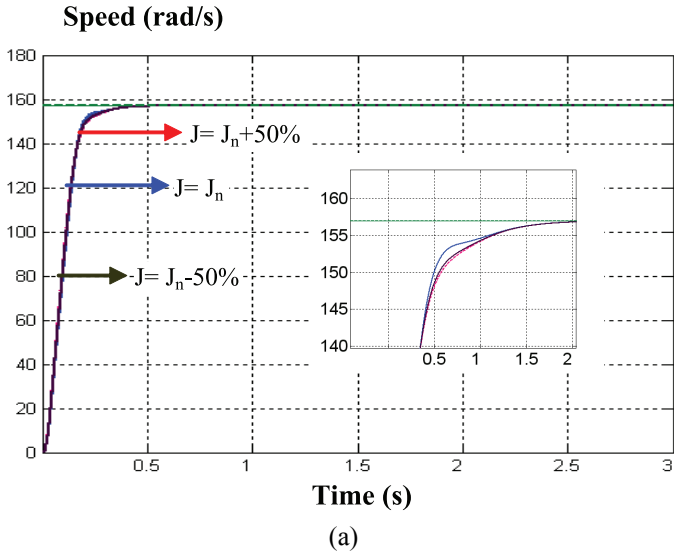


**Fig. 8** – Drive response under different inertia values:  
(a) DTC based IOFL, (b) Classical DTC.

**Table 1**  
*Induction motor parameters*

|                     |                          |
|---------------------|--------------------------|
| Rated power         | 4 KW                     |
| Pole pair           | P= 2                     |
| Nominal speed       | 1440 rpm                 |
| Stator inductance   | 0.1554 H                 |
| Rotor inductance    | 0.1568 H                 |
| Mutual inductance   | 0.15 H                   |
| Stator resistance   | 1.2 $\Omega$             |
| Rotor resistance    | 1.8 $\Omega$             |
| Machine inertia     | 0.07 kg.m <sup>2</sup>   |
| Viscous coefficient | 0.0 kg.m <sup>2</sup> /s |
| Rated frequency     | 50 Hz                    |

## 7 Conclusion

In this paper, we present a robust direct torque control method for voltage inverter – fed IM based on a space vector PWM scheme combined with input–output feedback linearization technique. The overall torque and flux control system was verified to be robust to the variations of motor mechanical and electrical parameters variations. Simulation studies were used to demonstrate the characteristics of the proposed method. It is shown that the proposed controller has better tracking performance and robustness against parameters variations as compared with the conventional direct torque control.

## 8 References

- [1] I. Takahashi, T. Noguchi: A New Quick-response and High Efficiency Control Strategy of an Induction Machine, IEEE Transaction on Industry Application, Vol. IA-22, No. 5, Sept. 1986, pp. 820 – 827.
- [2] S. Belkacem, F. Nacéri, R. Abdessemed: A Novel Robust Adaptive Control Algorithm and Application to DTC-SVM of AC Drives, Serbian Journal of Electrical Engineering, Vol. 7, No. 1, May 2010, pp. 21 – 40.
- [3] M. Romero, J.H. Braslavsky, M.I. Valla: Ripple Reduction in Direct Torque and Flux Control of Induction Motors via Sliding Modes, Latin American Applied Research, Vol. 37, No. 4, Oct. 2007, pp. 289 – 297.
- [4] S. Belkacem, F. Nacéri, R. Abdessemed: Robust Nonlinear Control for Direct Torque Control of Induction Motor Drive using Space Vector Modulation, Journal of Electrical Engineering, Vol. 10, No. 3, Sept. 2010, pp. 79 – 87.
- [5] M. Hajian, J. Soltani, G.R.A. Markadeh, S. Hosseinnia: Adaptive Nonlinear Direct Torque Control of Sensorless IM Drives with Efficiency Optimization, IEEE Transactions on Industrial Electronics, Vol. 57, No. 3, March 2010, pp. 975 – 985.
- [6] M. Hajian, J. Soltani, G.R.A. Markadeh, S. Hosseinnia: Input-output Feedback Linearization of Sensorless IM Drives with Stator and Rotor Resistances Estimation, Journal of Power Electronics, Vol. 9, No. 4, 2009, pp. 654 – 666.

- [7] S.X. Liu, M.Y. Wang, Y.G. Chen, S. Li: A Novel Fuzzy Direct Torque Control System for Three-level Inverter-fed Induction Machine, *International Journal of Automation and Computing*, Vol. 7, No. 1, Feb. 2010, pp. 78 – 85.
- [8] H.F.E. Soliman, E.M. Elbuluk: Direct Torque Control of a Three Phase Induction Motor using a Hybrid PI/Fuzzy Controller, *IEEE Industrial Application Conference*, New Orleans, LA, USA, Sept. 2007, pp. 1681 – 1685.
- [9] Z. Zhang, R. Tang, B. Bai, D. Xie: Novel Direct Torque Control Based on Space Vector Modulation with Adaptive Stator Flux Observer for Induction Motors, *IEEE Transactions on Magnetics*, Vol. 46, No. 8, Aug. 2010, pp. 3133 – 3136.
- [10] K.B. Lee, F. Blaabjerg: Improved Direct Torque Control for Sensorless Matrix Converter Drives with Constant Switching Frequency and Torque Ripple Reduction, *International Journal of Control, Automation, and Systems*, Vol. 4, No. 1, Feb. 2006, pp. 113 – 123.
- [11] H.A. Zarchi, G.R.A. Markadeh, J. Soltani: Direct Torque and Flux Regulation of Synchronous Reluctance Motor Drives based on Input–output Feedback Linearization, *Energy Conversion and Management*, Vol. 51, No. 1, Jan. 2010, pp. 71 – 80.
- [12] Y. Kumsuwan, W. Srirattanawichaikul, S. Premrudeepreechacharn: Reduction of Torque Ripple in Direct Torque Control for Induction Motor Drives using Decoupled Amplitude and Angle of Stator Flux Control, *ECTI Transactions on Electrical Engineering, Electronics and Communications*, Vol. 8, No. 2, Aug. 2010, pp. 187 – 196.
- [13] S. Belkacem, B. Zegueb, F. Naceri: Robust Non-linear Direct Torque and Flux Control of Adjustable Speed Sensorless PMSM Drive based on SVM using a PI Predictive Controller, *Journal of Engineering Science and Technology Review*, Vol. 3, No. 1, 2010, pp. 168 – 175.
- [14] J.J.E. Slotine, W. Li: *Applied Nonlinear Control*, Prentice-Hall, NJ, 1991.
- [15] A. Isidori: *Nonlinear Control Systems*, Springer-Verlag, NY, 1989.
- [16] J. Chiasson: Dynamic Feedback Linearization of the Induction Motors, *IEEE Transaction on Automatic Control*, Vol. 38, No. 10, Oct. 1993, pp. 1588 – 1594.
- [17] R. Marino, P. Tomei, C.M. Verrelli: An Adaptive Tracking Control from Current Measurements for Induction Motors with Uncertain Load Torque and Rotor Resistance, *Automatica*, Vol. 44, No. 10, Oct. 2008, pp. 2593 – 2599.
- [18] B.M. Dehkordi, A.F. Payam, M.N. Hashemnia, S.K. Sul: Design of an Adaptive Backstepping Controller for Doubly Fed Induction Machine Drives, *Journal of Power Electronics*, Vol. 9, No. 3, 2009, pp. 343 – 353.
- [19] R. Marino, P. Tomei, C.M. Verrelli: Adaptive Output Feedback Tracking Control for Induction Motors with Uncertain Load Torque and Resistances, *International Symposium on Power Electronics Electrical Drives Automation and Motion*, Pisa, Italia, June 2010, pp. 419 – 424.
- [20] A. Bentaallah, A. Meroufel, A. Bendaoud, A. Massoum, M.K. Fellah: Exact Linearization of an Induction Machine with Rotoric Flux Orientation, *Serbian Journal of Electrical Engineering*, Vol. 5, No. 2, Nov. 2008, pp. 217 – 227.